J. KSIAM **Vol.3**, No.2, 51-67, 1999

NUMERICAL SOLUTION OF A CONSTRICTED STEPPED CHANNEL PROBLEM USING A FOURTH ORDER METHOD

Paulo F. de A. Mancera* Roland Hunt†

Abstract

The numerical solution of the Navier-Stokes equations in a constricted stepped channel problem has been obtained using a fourth order numerical method. Transformations are made to have a fine grid near the sharp corner and a long channel downstream. The derivatives in the Navier-Stokes equations are replaced by fourth order central differences which result a 29-point computational stencil. A procedure is used to avoid extra numerical boundary conditions near the solid walls. Results have been obtained for Reynolds numbers up to 1000.

1 Introduction

We apply an wide fourth order numerical method for solving the Navier-Stokes equations to a constricted stepped channel problem. The constricted stepped channel problem considered consists of a sudden contraction (a forward-facing stepped channel, see Figure 1) and contains a re-entrant corner. Because of the difficulties associated with that corner this channel problem has been much studied.

Moffat [13] has studied the Stokesian flow near a re-entrant corner and has shown that the vorticity is singular. Bramley and Dennis [1] compare the Moffat expansion with their numerical solution near the corner for a branching channel problem and Hunt [9] compares the Moffat expansion along with other techniques for a constricted stepped channel problem. Dennis and Smith [4] solve a constricted stepped channel problem using diagonal grids near the corner. Holstein and Paddon [7] present a method which is based on using Moffat's expansion to produce finite difference stencils which take into account the nature of the singularity at the corner. Ma and Ruth [12] compare some of the techniques referenced above and others with their vorticity-circulation method.

There are many other calculations of this problem which use either the streamfunction-vorticity or the streamfunction formulation of the Navier-Stokes equations, and use various methods to solve the system of the non-linear equations. We will cite a few. Dennis and Smith [4] use the streamfunction-vorticity formulation of the Navier-Stokes equations discretisating the streamfunction by second order central differences and the vorticity equation by second order central differences which incorporate the Dennis-Hudson artificial viscosity and the resulting system of equations is solved using an

Keywords: Navier-Stokes equations, fourth order numerical method, streamfunction formulation.
AMS Subject Classification: 65N06

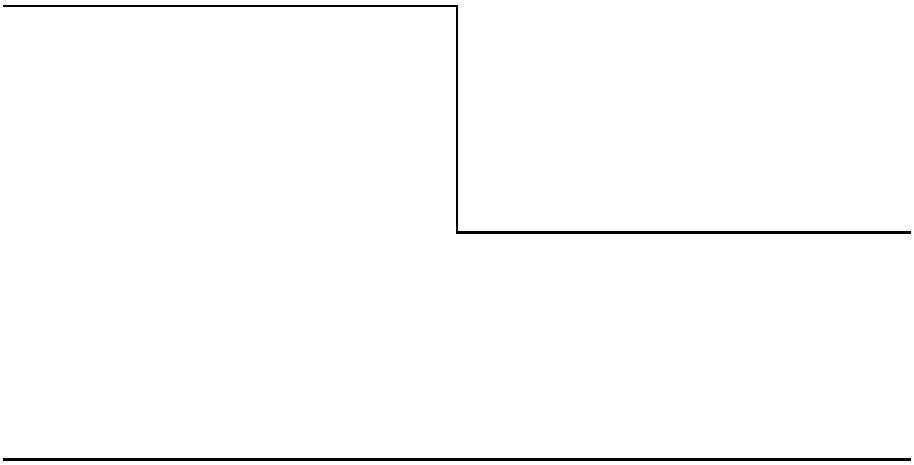

Figure 1: Stepped channel.

SOR iteration. Huang and Seymour [8] use the interior constraint method for solving the streamfunction-vorticity formulation and again an SOR iteration is used to solve the system of equations. Hunt [9] solves the streamfunction formulation using second order central differences and Newton method is used to solve the resulting system of equations. Karageorghis and Phillips [11] solve the streamfunction formulation using the Chebyshev spectral element method and the resulting system of equations is solved by Newton method. Finally we observe that the computational domain for the constricted stepped channel problem is L-shaped region. This causes considerable difficulties in applying a 29-point computational stencil near the re-entrant corner. However the main difficulty with the constricted stepped channel problem is that the flow at the re-entrant corner is singular, that is the second and higher derivatives of the streamfunction are singular.

2 Forward-facing stepped channel

Let us consider a channel problem with walls at $y = \pm 1$ for $x < 0$, $y = \pm\frac{1}{2}$ for $x > 0$ and $\frac{1}{2} \leq |y| \leq 1$ for $x = 0$. Due to symmetry the problem is solved for $y \geq 0$ (see Figure 1). The governing equations for this channel problem are given by the Navier-Stokes equations

$$\frac{\partial^2 \psi}{\partial x^2} + \frac{\partial^2 \psi}{\partial y^2} = -\zeta \tag{1}$$

$$\frac{\partial^2\zeta}{\partial x^2}+\frac{\partial^2\zeta}{\partial y^2} = Re\left(\frac{\partial\psi}{\partial y}\frac{\partial\zeta}{\partial x}-\frac{\partial\psi}{\partial x}\frac{\partial\zeta}{\partial y}\right) \tag{2}$$

where Re is the Reynolds number and the boundary conditions are

$$\begin{aligned}
\psi &= 1, \quad \frac{\partial\psi}{\partial y}=0 \text{ on } y=1,\ x\le 0, \quad \text{and} \quad y=\frac{1}{2},\ x\ge 0\\
\psi &= 1, \quad \frac{\partial\psi}{\partial x}=0 \text{ on } x=0, \frac{1}{2}\le y\le 1\\
\psi &= 0, \quad \frac{\partial^2\psi}{\partial y^2}=0 \text{ on } y=0\\
\psi &\to \frac{3}{2}y-\frac{1}{2}y^3, \quad \zeta\to 3y \quad \text{as} \quad x\to-\infty,\\
\psi &\to 3y-4y^3, \quad \zeta\to 24y \quad \text{as} \quad x\to+\infty
\end{aligned} \tag{3}$$

where Poiseuille flow has been assumed far upstream and far downstream.

Substituting equation (1) into equation (2) gives

$$\frac{\partial^4\psi}{\partial x^4}+2\frac{\partial^4\psi}{\partial x^2\partial y^2}+\frac{\partial^4\psi}{\partial y^4} = Re\left(\frac{\partial\psi}{\partial y}\left(\frac{\partial^3\psi}{\partial x^3}+\frac{\partial^3\psi}{\partial x\partial y^2}\right)-\frac{\partial\psi}{\partial x}\left(\frac{\partial^3\psi}{\partial y\partial x^2}+\frac{\partial^3\psi}{\partial y^3}\right)\right) \tag{4}$$

which is called the streamfunction formulation for the steady incompressible Navier-Stokes equations

Because of the need of finer grid near the sharp corner we consider transformations given by

$$\xi=f(\xi), \quad \eta=g(\eta) \tag{5}$$

and hence the governing equations are given by

$$\mathcal{D}\psi = -\zeta \tag{6}$$

$$\mathcal{D}\zeta = \frac{Re}{f'g'}\left(\frac{\partial\zeta}{\partial\xi}\frac{\partial\psi}{\partial\eta}-\frac{\partial\zeta}{\partial\eta}\frac{\partial\psi}{\partial\xi}\right) \tag{7}$$

where

$$\mathcal{D}\equiv\frac{1}{f'^2}\frac{\partial^2}{\partial\xi^2}-\frac{f''}{f'^3}\frac{\partial}{\partial\xi}+\frac{1}{g'^2}\frac{\partial^2}{\partial\eta^2}-\frac{g''}{g'^3}\frac{\partial}{\partial\eta} \tag{8}$$

We have chosen the same transformations given by Hunt [9], that is

$$x = f(\xi)=\frac{\Delta x_0}{k}\sinh(k\,\xi) \tag{9}$$

$$y = g(\eta)=\eta+\frac{1}{2\pi}(1-\Delta y_0)\sin(2\,\pi\,\eta) \tag{10}$$

where $h\,\Delta x_0$ and $h\,\Delta y_0$ are the dimensions of a cell in the x–y plane near the corner, k is a parameter determined by the position of the upstream boundary and h is the grid size. Figure 2 shows an example of a non-uniform grid placed on the channel.

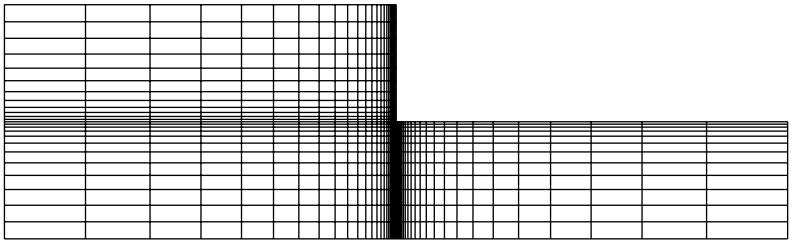

Figure 2: Forward-facing stepped channel: grid mesh.

3 THE STREAMFUNCTION FORMULATION ON A NON-UNIFORM GRID

Mancera [2] and Mancera and Hunt [3] have used a procedure to deal with the streamfunction formulation of the Navier-Stokes equations on a non-uniform grid which consists of

1. Discretise equations (6) and (7) using fourth order central differences.
2. Eliminate $\zeta_{i,j}$ from these equations.
3. Obtain a computational stencil with 29 points.

We will obtain the full expression for the streamfunction formulation of the Navier-Stokes equations to analyse this constricted stepped problem since after discretising the equation we will have a 29-point computational stencil, instead of the 33-point computational stencil resulting from the procedure cited above (step 2). Writing equation (6) as

$$\zeta = -\frac{1}{f'^2}\frac{\partial^2\psi}{\partial\xi^2} + \frac{f''}{f'^3}\frac{\partial\psi}{\partial\xi} - \frac{1}{g'^2}\frac{\partial^2\psi}{\partial\eta^2} + \frac{g''}{g'^3}\frac{\partial\psi}{\partial\eta} \tag{11}$$

and then calculating $\dfrac{\partial\zeta}{\partial\xi}$, $\dfrac{\partial\zeta}{\partial\eta}$, $\dfrac{\partial^2\zeta}{\partial\xi^2}$ e $\dfrac{\partial^2\zeta}{\partial\eta^2}$ we obtain, after substituting these derivatives in equation (7),

$$\begin{aligned}
- & \frac{1}{f'^4}\frac{\partial^4\psi}{\partial\xi^4} - \frac{1}{g'^4}\frac{\partial^4\psi}{\partial\eta^4} - \frac{2}{f'^2g'^2}\frac{\partial^4\psi}{\partial\xi^2\partial\eta^2} + \frac{6f''}{f'^5}\frac{\partial^3\psi}{\partial\xi^3} + \frac{6g''}{g'^5}\frac{\partial^3\psi}{\partial\eta^3} + \frac{2g''}{f'^2g'^3}\frac{\partial^3\psi}{\partial\xi^2\partial\eta} \\
+ & \frac{2f''}{g'^2f'^3}\frac{\partial^3\psi}{\partial\eta^2\partial\xi} + \frac{4f'''f' - 15f''^2}{f'^6}\frac{\partial^2\psi}{\partial\xi^2} + \frac{4g'''g' - 15g''^2}{g'^6}\frac{\partial^2\psi}{\partial\eta^2} + \frac{2g''f''}{(f'g')^3}\frac{\partial^2\psi}{\partial\eta\partial\xi} \\
+ & \frac{f''''f'^2 - 10f'f''f''' + 15f''^3}{f'^7}\frac{\partial\psi}{\partial\xi} + \frac{g''''g'^2 - 10g'g''g''' + 15g''^3}{g'^7}\frac{\partial\psi}{\partial\eta} \\
- & \frac{Re}{f'g'}\left(\frac{\partial\psi}{\partial\eta}\left(\frac{3f''}{f'^3}\frac{\partial^2\psi}{\partial\xi^2} - \frac{1}{f'^2}\frac{\partial^3\psi}{\partial\xi^3} + \frac{f'''f' - 3f''^2}{f'^4}\frac{\partial\psi}{\partial\xi} - \frac{1}{g'^2}\frac{\partial^3\psi}{\partial\xi\partial\xi^2} + \frac{g''}{g'^3}\frac{\partial^2\psi}{\partial\xi\partial\eta}\right)\right.
\end{aligned}$$

$$- \frac{\partial\psi}{\partial\xi}\left(-\frac{1}{f'^2}\frac{\partial^3\psi}{\partial\eta\partial\xi^2}+\frac{f''}{f'^3}\frac{\partial^2\psi}{\partial\eta\partial\xi}+\frac{3g''}{g'^3}\frac{\partial^2\psi}{\partial\eta^2}-\frac{1}{g'^2}\frac{\partial^3\psi}{\partial\eta^3}+\frac{g'''g'-3g''^2}{g'^4}\frac{\partial\psi}{\partial\eta}\right)=0 \quad (12)$$

Equation (12) is the streamfunction formulation of the Navier-Stokes equations on a non-uniform grid considering the transformations given in (5). Finally, we observe that if $f' = g' = 1$ in (12) then the expression (4) is obtained.

4 DISCRETISATION OF THE EQUATION

We set a uniform grid on the computational domain with grid size h in both directions ξ and η. If $\psi_{i,j}$ denotes an aproximation to ψ at position (i,j) then the derivatives on the ξ-direction are approximated by fourth order centre differences, that is,

$$\begin{aligned}
\frac{\partial\psi}{\partial x} &= \frac{1}{12h}\left(-\psi_{i+2,j}+8\psi_{i+1,j}-8\psi_{i-1,j}+\psi_{i-2,j}\right)+O\left(h^4\right)\\
\frac{\partial^2\psi}{\partial x^2} &= \frac{1}{12h^2}\left(-\psi_{i+2,j}+16\psi_{i+1,j}-30\psi_{i,j}+16\psi_{i-1,j}-\psi_{i-2,j}\right)+O\left(h^4\right) \quad (13)\\
\frac{\partial^3\psi}{\partial x^3} &= \frac{1}{8h^3}\left(-\psi_{i+3,j}+8\psi_{i+2,j}-13\psi_{i+1,j}+13\psi_{i-1,j}-8\psi_{i-2,j}+\psi_{i-3,j}\right)+O\left(h^4\right)\\
\frac{\partial^4\psi}{\partial x^4} &= \frac{1}{6h^4}(-\psi_{i+3,j}+12\psi_{i+2,j}-39\psi_{i+1,j}+56\psi_{i,j}-39\psi_{i-1,j}\\
&+ 12\psi_{i-2,j}-\psi_{i-3,j})+O\left(h^4\right)
\end{aligned}$$

The mixed derivatives are evaluated in the programme using a *do* loop. For example, $\dfrac{\partial^3\psi}{\partial\xi\partial\eta^2}$ is approximated by

$$\begin{aligned}
a_l &= \frac{1}{12h}\left(-\psi_{i+2,j+l}+8\psi_{i+1,j+l}-8\psi_{i-1,j+l}+\psi_{i-2,j+l}\right),\quad l=-2,-1,0,1,2\\
\frac{\partial^3\psi}{\partial\xi\partial\eta^2} &\simeq \frac{1}{12h^2}\left(-a_2+16a_1-30a_0+16a_{-1}-a_{-2}\right) \quad (14)
\end{aligned}$$

which gives a 5×5-computational stencil. Equation (12) is discretised by formulas (13) and (14) to result the 29-point-computational stencil as shown in Figure 3.

The application of the 29-point computational stencil to this constricted stepped channel problem is not straightforward because of the difficulties to deal with fictitious points near the sharp corner (singular point). To understand the difficulties let us consider two situations of calculations near the sharp corner as illustrated in Figure 4. Applying the computational stencil with 29 points at positions denoted by $\oplus$ we note that both calculations use common fictitious points, but the behaviour of the flow before the corner is different from the behaviour after the corner. Hence the four fictitious nodes near the corner have two values for the streamfunction each depending whether the centre of the computational stencil is before or after the corner. To overcome these difficulties we have not used fictitious points at the solid walls in the calculations. If we

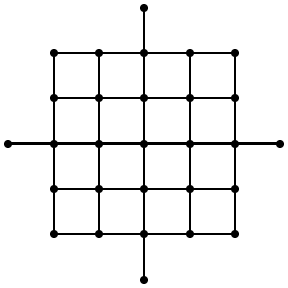

Figure 3: Computational stencil with 29 points.

apply the 13-point computational stencil* at the interior points next to the boundary and the 29-point computational stencil at all other interior points then we only require the value of ψ at a single point, denoted by $\psi_\star$, outside the boundary. This can be eliminated using the derivative boundary condition at the wall given by

$$\frac{\partial \psi}{\partial n} = 0 \tag{15}$$

where $\dfrac{\partial \psi}{\partial n}$ is the normal derivative. Using fourth order discretisation we can approximate this by

$$\frac{\partial \psi}{\partial n} \simeq \frac{1}{12h}\left(3\psi_\star + 10\psi_0 - 18\psi_1 + 6\psi_2 - \psi_3\right) = 0 \tag{16}$$

where the subscripts 0, 1, 2 and 3 denote, respectively, a point on the boundary and $j = 1, 2, 3$ the j-th internal grid point along the inward normal from 0, and $\star$ a point outside the boundary. From (16) we obtain that

$$\psi_\star = \frac{1}{3}\left(-10\psi_0 + 18\psi_1 - 6\psi_2 + \psi_3\right) \tag{17}$$

which can be used to remove the fictitious point from the computational stencils with 13 and 29 points and then there are no fictitious points used in the calculations. Our use of applying the 13-point computational stencil next to the boundary differs slightly from Henshaw's procedure (see Henshaw [5] and Henshaw et. al. [6]) where that computational stencil is applied on the boundary, but the method can be shown to be still fourth order accurate (Hunt, private communication).

Using these ideas we have set up a procedure (see Figure 5 for positions of calculations near the re-entrant corner) to discretise the governing equation in the computational domain. The procedure is as follows. Let us consider an $N_1 \times M_1$ grid before

*This computational stencil is obtained by discretising the governing equation by second order central differences.

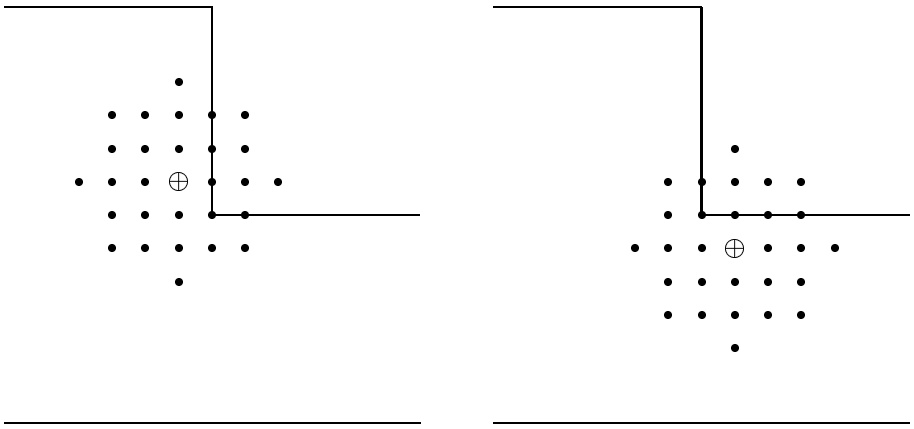

Figure 4: Computational stencils near the re-entrant corner.

the sharp corner and an $N_2 \times M_2$, where $M_2 = \dfrac{M_1}{2}$ after it, where the grid vertices are (i, j), $i = -N_1, -N_1+1, \ldots, -1, 0, 1, \ldots, N_2$, $j = 0, 1, \ldots, M$, where $M = M_1$ for $i \leq 0$ and $M = M_2$ for $i > 0$. Then

1. At points $j = M_1 - 1$ for $-N_1 + 1 \leq i \leq -2$ and $j = M_2 - 1$ for $1 \leq i \leq N_2 - 1$ we apply a computational stencil with 13 points (second order accurate) with all fictitious points replaced by (17), that is $\psi_\star = \dfrac{1}{3}(-10\psi_{i,M_1} + 18\psi_{i,M_1-1} - 6\psi_{i,M_1-2} + \psi_{i,M_1-3})$ at $j = M_1 - 1$ and $\psi_\star = \dfrac{1}{3}(-10\psi_{i,M_2} + 18\psi_{i,M_2-1} - 6\psi_{i,M_2-2} + \psi_{i,M_2-3})$ at $j = M_2 - 1$. In Figure 5 these points are indicated by **1**.

2. At $i = -1$ for $M_2 + 1 \leq j \leq M_1 - 2$ we apply a 13-point computational stencil with fictitious points substituted by $\psi_\star = \dfrac{1}{3}(-10\psi_{0,j} + 18\psi_{-1,j} - 6\psi_{-2,j} + \psi_{-3,j})$ (see **2** in Figure 5).

3. At grid position $(-1, M_1 - 1)$ we apply a computational stencil with 13 points, where to eliminate fictitious points in both axis directions we apply similar expressions to $\psi_\star$ as those given in the two items above (see **3** in Figure 5).

4. At grid positions $(-1, M_2)$, $(-1, M_2 - 1)$ and $(0, M_2 - 1)$ we apply a computational stencil with 13 points (see **4** in Figure 5).

5. At positions $j = M_1 - 2$ for $-N_1 + 1 \leq i \leq -3$ and $j = M_2 - 2$ for $1 \leq i \leq N_2 - 1$ we apply a computational stencil with 29 points (fourth order accurate), where $\psi_\star = \dfrac{1}{3}(-10\psi_{i,k} + 18\psi_{i,k-1} - 6\psi_{i,k-2} + \psi_{i,k-3})$ with k either M_1 or M_2 is used to eliminate fictitious points (see **5** in Figure 5).

6. At $i = -2$ for $M_2 + 1 \leq j \leq M_1 - 3$ the 29-point computational stencil is applied with all fictitious points substituted by the same expression given in the second item (see **6** in Figure 5).

7. At position $(-2, M_1 - 2)$ we apply a computational stencil with 29 points with all fictitious points in both directions eliminated using $\psi_\star$ given in the two preceding items (see **7** in Figure 5).

8. To other interior points we apply a computational stencil with 29 points. In Figure 5 they are indicated by **8**.

9. On solid walls we have $\psi_{i,j} = 1$ and along the line of symmetry $\psi_{i,0} = 0$, $\psi_{i,-1} = -\psi_{i,1}$ and $\psi_{i,-2} = -\psi_{i,2}$.

10. At the ends of the channel we have set $\psi_{0,j} = \dfrac{jh}{2}(3 - jh)$, $\psi_{N,j} = \left(3jh - 4(jh)^3\right)$, $-\psi_{-N_1+2,j} + 16\psi_{-N_1+1,j} - 30\psi_{-N_1,j} + 16\psi_{-N_1-1,j} - \psi_{-N_1-2,j} = 0$ and $-\psi_{-N_2+2,j} + 16\psi_{-N_2+1,j} - 30\psi_{-N_2,j} + 16\psi_{-N_2-1,j} - \psi_{-N_2-2,j} = 0$.

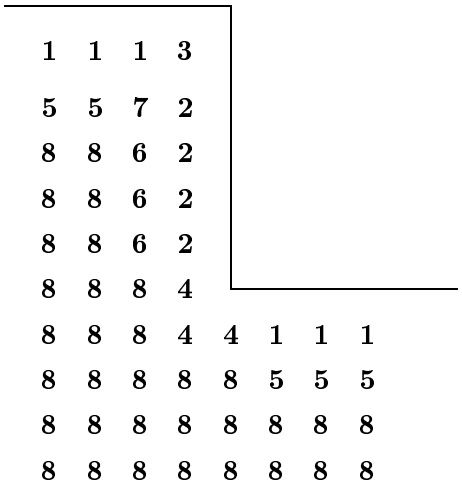

Figure 5: Stepped channel: positions of the calculations near the solid walls.

5 NUMERICAL SOLUTION AND ACCURACY

The system of algebraic equations resulting from the discretizations is solved by Newton method which is described in Hunt [9, 10] and Mancera and Hunt [3]. The numerical solution is obtained on an $N \times M$ grid and in order to estimate the error in these results we obtain a second solution on a $N/2 \times M/2$ grid for comparison. Suppose, at a common location, the numerical solution is ϕ_F on the original fine grid and ϕ_M on the coarser grid and, if further ϕ is the exact solution at this point, then since the methods are fourth order we have

$$\phi - \phi_F \simeq Kh^4, \quad \phi - \phi_M \simeq K(2h)^4 \tag{18}$$

for some constant K. Eliminating ϕ we obtain an estimate for the error E_F on the fine grid ($\simeq Kh^4$) as

$$E_F \simeq \frac{\phi_F - \phi_M}{15} \tag{19}$$

The errors are estimated as follows

$$\texttt{RMS}: \; ||\psi^F - \psi^M||_2 = \left(\frac{1}{N}\sum\left(\psi_{ij}^F - \psi_{ij}^M\right)^2\right)^{1/2} \tag{20}$$

$$\texttt{maximum}: \; ||\psi^F - \psi^M||_\infty = \max_{ij} |\psi_{ij}^F - \psi_{ij}^M| \tag{21}$$

where N is the number of points on the computational space, $\psi_{i,j}^F$ and ψ_{ij}^M, are, respectively the numerical solution at (i, j) on the fine and coarser grids.

6 Results for the stepped channel

We numerically solve the flow in the forward-facing stepped channel problem using the 29-point computational stencil together with boundary data in which all fictitious points are eliminated. We consider the elimination of the fictitious points to be the best approach to this problem. Let us explain step by step the process of discretisation. First, the Navier-Stokes equations (1) and (2) are transformated in equations (6) and (7), where the coordinate transformations are given by equations (9) and (10). Second, equations (6) and (7) are written in the streamfunction formulation alone (equation (12)) and then discretised by fourth order central differences to obtain a 29-point computational stencil. Third, equation (12) is also discretised using second order central differences to obtain a 13-point computational stencil which is applied adjacent to the walls. Fourth, we apply a procedure to eliminate all fictitious points at the solid walls. The results are presented both for a uniform grid and for a non-uniform.

For the uniform grid we have set the upstream boundary at $x = -2$ and the downstream boundary at $x = 2$, where the number of points on the fine grid is 96 in the y-direction before the corner. The maximum and RMS errors are shown in Tables [†]

[†] The notation $a(-b)$ means $a \times 10^{-b}$.

Table 1: Maximum errors on a uniform grid.

	Methods		
	Fourth order method	Second order method	
Re	ψ errors	ψ errors	Ratio
0	1.50(-4)	8.00(-4)	5.33
1	1.55(-4)	8.32(-4)	5.37
10	1.86(-4)	1.04(-3)	5.59
50	2.24(-4)	1.53(-3)	6.83
100	2.32(-4)	1.84(-3)	7.93
250	4.35(-4)	2.26(-3)	5.20
500	1.97(-3)	2.30(-3)	1.17

Table 2: RMS errors on a uniform grid.

	Methods		
	Fourth order method	Second order method	
Re	ψ errors	ψ errors	Ratio
0	2.86(-5)	1.41(-4)	4.93
1	2.81(-5)	1.42(-4)	5.05
10	2.68(-5)	1.54(-4)	5.75
50	2.91(-5)	1.70(-4)	5.84
100	3.14(-5)	1.75(-4)	5.57
250	5.45(-5)	2.55(-4)	4.68
500	3.56(-4)	4.46(-4)	1.25

1 and 2, respectively. We note from both tables that the results given by the fourth order method are not much more accurate than their second order counterparts where for all Re the errors for the fourth order method are less than 8 times smaller than their second order equivalent.

Now we analyse the results where fictitious points are not used on the solid walls. The upstream position is at $x = -2$ and the downstream position is either at $x \simeq 100$ or at $x \simeq 1000$. In the numerical simulations we have chosen $\Delta x_0 = \Delta y_0 = 0.025$ and $\Delta x_0 = 0.01$ and $\Delta y_0 = 0.025$ on the coarser grid.

In Tables 3 and 4 we present results for the fourth and second order methods on a non-uniform grid where the upstream position is at $x = -2$, the downstream position at $x \simeq 109$, the value of the parameter k in equation (9) is 2.9973 and $\Delta x_0 = \Delta y_0 = 0.025$. The number of points in the ξ-direction is 80 and in the η-direction 24 on the coarser grid. Comparing the results given in Tables 3 and 4 with those given in Tables 1 and 2 we have obtained results up to $Re = 1000$, even though for the fourth order method Newton method has failed to converge after 10 iterations. For the fourth order numerical method the errors on a non-uniform grid are smaller than the errors on a

Table 3: Maximum errors and ratio between errors for the upstream position at $x = -2$, downstream position at $x \simeq 109$ and $\Delta x_0 = \Delta y_0 = 0.025$.

	Methods		
	Fourth order method	Second order method	
Re	ψ errors	ψ errors	Ratio
0	8.81(-5)	9.60(-4)	10.90
1	9.11(-5)	9.13(-4)	10.02
10	1.10(-4)	6.28(-4)	5.71
50	1.43(-4)	7.02(-4)	4.91
100	1.57(-4)	9.53(-4)	6.07
125	1.62(-4)	1.04(-3)	6.42
250	1.89(-4)	1.34(-3)	7.09
500	3.99(-4)	1.64(-3)	4.11
750	9.16(-4)	2.84(-3)	3.10
1000	—	4.79(-3)	—

uniform grid for all Reynolds numbers. The ratio between the errors are less than 11 for the maximum erros and less than 13 for the RMS errors.

The results for the situation upstream position at $x = -2$ and downstream position at $x \simeq 1033$ are given in Tables 5 and 6, where the number of points in the ξ-direction is 98 and in the η-direction is 24 on the coarser grid. We have obtained results for Reynolds number up to 1000 and for both fourth and second order numerical methods. Comparing the maximum and RMS errors given in Tables 5 and 6 with their counterparts given in Tables 3 and 4 we observe the same results for the maximum errors and the RMS errors are smaller for the downstream position $x \simeq 1033$ since the flow changes very slowly after the the sharp corner. Again the ratios between the errors from the second and fourth order methods are, respectively, less than 12 and less than 14 for the maximum and RMS errors.

We have also analysed the constricted stepped channel problem for the same upstream and downstream positions but considering $\Delta x_0 = 0.01$ and $\Delta y_0 = 0.025$. We have chosen these values after many numerical experimentations, since the Newton method employed has not converged for some values of Δx_0 and Δy_0. For the upstream position at $x = -2$ and downstream position at $x \simeq 142$ the number of points in the ξ-direction is 72 and in the η-direction 24 on the coarser grid and $k = 4.2638$. The maximum errors (see Table 7) range from 4.78×10^{-5} to 3.12×10^{-4} for the fourth order method and the ratios between the errors from the second and fourth order methods are less than 25 for all Reynolds numbers. For the fourth order method the RMS errors given in Table 8 range from 6.02×10^{-5} to 1.28×10^{-5} and again the ratios between the errors are less than 25. The fourth order method did not converge after 10 iterations to $Re = 1000$ on the coarser grid. Comparing the errors for the fourth order method given in Tables 3 and 4 with those given in Tables 7 and 8 we observe that both maximum and RMS errors are smaller for $\Delta x_0 = 0.01$ and $\Delta y_0 = 0.025$.

Table 4: RMS errors and ratio between errors for the upstream position at $x = -2$, downstream position at $x \simeq 109$ and $\Delta x_0 = \Delta y_0 = 0.025$.

	Methods		
	Fourth order method	Second order method	
Re	ψ errors	ψ errors	Ratio
0	2.03(-5)	2.59(-4)	12.76
1	2.04(-5)	2.49(-4)	12.21
10	2.10(-5)	1.89(-4)	9.00
50	2.33(-5)	1.34(-4)	5.75
100	2.60(-5)	1.35(-4)	5.19
125	2.67(-5)	1.37(-4)	5.13
250	3.15(-5)	1.49(-4)	4.73
500	6.85(-5)	1.70(-4)	2.48
750	1.71(-4)	5.14(-4)	3.01
1000	—	6.52(-4)	—

Table 5: Maximum errors and ratio between errors for the upstream position at $x = -2$, downstream position at $x \simeq 1033$ and $\Delta x_0 = \Delta y_0 = 0.025$.

	Methods		
	Fourth order method	Second order method	
Re	ψ errors	ψ errors	Ratio
0	8.81(-5)	9.60(-4)	10.90
1	9.11(-5)	9.13(-4)	10.02
10	1.10(-4)	6.28(-4)	5.71
50	1.43(-4)	7.02(-4)	4.91
100	1.57(-4)	9.53(-4)	6.07
125	1.62(-4)	1.04(-3)	6.42
250	1.89(-4)	1.34(-3)	7.09
500	3.99(-4)	1.64(-3)	4.11
750	9.26(-4)	1.72(-3)	1.86
1000	1.33(-3)	2.00(-3)	1.50

Table 6: RMS errors and ratio between errors for the upstream position at $x = -2$, downstream position at $x \simeq 1033$ and $\Delta x_0 = \Delta y_0 = 0.025$.

	Methods		
	Fourth order method	Second order method	
Re	ψ errors	ψ errors	Ratio
0	1.84(-5)	2.44(-4)	13.26
1	1.85(-5)	2.36(-4)	12.76
10	1.90(-5)	1.85(-4)	9.74
50	2.13(-5)	1.40(-4)	6.57
100	2.35(-5)	1.41(-4)	6.00
125	2.42(-5)	1.42(-4)	5.87
250	2.85(-5)	1.52(-4)	5.33
500	6.19(-5)	1.70(-4)	2.75
750	1.60(-4)	2.23(-4)	1.39
1000	2.28(-4)	3.01(-4)	1.32

Table 7: Maximum errors and ratio between errors for the upstream position at $x = -2$, downstream position at $x \simeq 142$ and $\Delta x_0 = 0.01$ and $\Delta y_0 = 0.025$.

	Methods		
	Fourth order method	Second order method	
Re	ψ errors	ψ errors	Ratio
0	4.78(-5)	1.16(-3)	24.27
1	4.94(-5)	1.10(-3)	22.27
10	6.05(-5)	7.49(-4)	12.38
50	8.33(-5)	6.82(-4)	8.19
100	9.72(-5)	5.10(-4)	5.25
125	1.00(-4)	5.37(-4)	5.37
250	1.03(-4)	6.82(-4)	6.62
500	1.38(-4)	1.03(-3)	7.46
750	3.12(-4)	6.98(-3)	22.37
1000	—	5.37(-2)	—

Table 8: RMS errors and ratio between errors for the upstream position at $x = -2$, downstream position at $x \simeq 142$ and $\Delta x_0 = 0.01$ and $\Delta y_0 = 0.025$.

	Methods		
	Fourth order method	Second order method	
Re	ψ errors	ψ errors	Ratio
0	1.28(-5)	3.05(-4)	23.83
1	1.31(-5)	2.96(-4)	22.60
10	1.50(-5)	2.18(-4)	14.53
50	1.82(-5)	1.23(-4)	6.76
100	2.05(-5)	1.18(-4)	5.76
125	2.10(-5)	1.18(-4)	5.62
250	1.95(-5)	1.23(-4)	6.31
500	2.63(-5)	2.05(-4)	7.80
750	6.02(-5)	1.25(-3)	20.76
1000	—	9.74(-3)	—

In Tables 9 and 10 we present errors for the downstream position at $x \simeq 1199$ with the number of points in the ξ-position equal to 84. We have obtained results up to $Re = 1000$ for the fourth order method and up to $Re = 750$ for the second order method. Again the ratios between the errors are less than 25 for both maximum and RMS errors and the RMS errors are slightly smaller than the RMS errors for the channel with the downstream position at $x \simeq 142$.

Comparing both situations of channel length and grid refining we observe that the upstream position $x = -2$, downstream position $x \simeq 1199$, $\Delta x_0 = 0.01$ and $\Delta y_0 = 0.025$ have given the best results for the fourth order numerical method, although the ratio between the errors for all situations analysed has indicated that the fourth order numerical method is not much more accurate than the second order method for this channel problem.

7 Conclusions

We have analysed a fourth order numerical method for solving the Navier-Stokes equations for the constricted stepped channel. We have set a transformation which gives a fine grid near the sharp corner and a long channel downstream. For the most situations we have obtained results for Reynolds numbers up to 1000. Due to difficulties to deal with the solution near the sharp corner we have used a procedure which gives no fictitious points at the solid walls. For this channel problem the fourth order numerical method is not much more accurate than the second order method, but we must note that ψ has singular derivatives at the sharp corner which influences the solution, as can be observed in Mancera and Hunt [3] where a channel problem with gradual and smooth constriction is solved.

Table 9: Maximum errors and ratio between errors for the upstream position at $x = -2$, downstream position at $x \simeq 1199$ and $\Delta x_0 = 0.01$ and $\Delta y_0 = 0.025$.

	Methods		
	Fourth order method	Second order method	
Re	ψ errors	ψ errors	Ratio
0	4.78(-5)	1.16(-3)	24.27
1	4.94(-5)	1.10(-3)	22.27
10	6.05(-5)	7.49(-4)	12.38
50	8.33(-5)	3.95(-4)	4.74
100	9.72(-5)	5.10(-4)	5.25
125	1.00(-4)	5.37(-4)	5.37
250	1.03(-4)	6.82(-4)	6.62
500	1.38(-4)	1.03(-3)	7.46
750	3.11(-4)	1.03(-3)	3.31
1000	5.64(-4)	—	—

Table 10: RMS errors and ratio between errors for the upstream position at $x = -2$, downstream position at $x \simeq 1199$ and $\Delta x_0 = 0.01$ and $\Delta y_0 = 0.025$.

	Methods		
	Fourth order methods	Second order methods	
Re	erros ψ	erros ψ	Ratio
0	1.19(-5)	2.89(-4)	24.29
1	1.22(-5)	2.81(-4)	23.03
10	1.39(-5)	2.11(-4)	15.18
50	1.69(-5)	1.30(-4)	7.69
100	1.90(-5)	1.25(-4)	6.58
125	1.95(-5)	1.25(-4)	6.41
250	1.80(-5)	1.30(-4)	7.22
500	2.43(-5)	1.99(-4)	8.19
750	5.59(-5)	3.94(-4)	4.23
1000	9.31(-5)	—	—

ACKNOWLEDGEMENT

The first author was supported by FAPESP–Fundação de Amparo à Pesquisa do Estado de São Paulo under grant 1996-9530-5.

References

[1] J. S. Bramley and S. C. R. Dennis, *The numerical solution of two-dimensional flow in a branching channel*, Comput Fluids, 12–4 (1984), pp. 339–355.

[2] P. F. de A. Mancera, *Fourth Order Numerical Methods For Solving The Navier-Stokes Equations in Two Dimensions*, PhD thesis, University of Strathclyde, 1996.

[3] P. F. de A. Mancera and R. Hunt, *Fourth order method for solving the Navier-Stokes equations in a constricting channel*, Int. J. Numer. Methods Fluids, 25 (1997), pp. 1119–1135.

[4] S. C. R. Dennis and F. T. Smith, *Steady flow through a channel with a symmetrical constriction in the form of a step*, Proc. R. Soc. Lond., A. 372 (1980), pp. 393–414.

[5] W. D. Henshaw, *A fourth-order accurate method for the incompressible Navier-Stokes equations on overlapping grids*, J. Comput. Phys., 113 (1994), pp. 13–25.

[6] W. D. Henshaw, H.-O. Kreiss, and L. G. M. Reyna, *A fourth-order-accurate difference approximation for the incompressible Navier-Stokes equations*, Comput Fluids, 23-4 (1994), pp. 575–593.

[7] H. Holstein and D. J. Paddon, *A singular finite difference treatment of re-entrant corner flow*, J. Non-Newtonian Fluid Mech., 8 (1981), pp. 81–93.

[8] H. Huang and B. R. Seymour, *A finite difference method for flow in a constricted channel*, technical report 93-167, University of British Columbia, 1993.

[9] R. Hunt, *The numerical solution of the laminar flow in a constricted channel at moderately high Reynolds number using Newton iteration*, Int. J. Numer. Methods Fluids, 11 (1990), pp. 247–259.

[10] ——, *The numerical solution of the flow in a general bifurcating channel at moderately high Reynolds number using boundary-fitted co-ordinates, primitive variables and Newton iteration*, Int. J. Numer. Methods Fluids, 17 (1993), pp. 711–729.

[11] A. Karageorghis and T. N. Phillips, *Chebyshev spectral collocation methods for laminar flow through a channel contraction*, J. Comput. Physics, 84 (1989), pp. 114–133.

[12] H. Ma and D. W. Ruth, *A new scheme for vorticity computations near a sharp corner*, Comput Fluids, 23–1 (1994), pp. 23–38.

[13] M. K. Moffat, *Viscous and resistive eddies near a sharp corner*, J. Fluid Mech., 18 (1964), pp. 1–59.

Departamento de Bioestatística
Instituto de Biociências–UNESP
CP 510
18618-000 Botucatu–Brazil
e-mail: pmancera@ibb.unesp.br

Department of Mathematics
University of Strathclyde
26 Richmond Street
G1 1XH Glasgow–Scotland
e-mail: r.hunt@strath.ac.uk